MACROSCOPIC FLUID FLOW OF LOW GRADIENT MAGNETOPHORESIS THROUGH CELLULOSE MATRIX

JAMES LAW KAH CHUN

UNIVERSITI SAINS MALAYSIA

2022

MACROSCOPIC FLUID FLOW OF LOW GRADIENT MAGNETOPHORESIS THROUGH CELLULOSE MATRIX

JAMES LAW KAH CHUN

Thesis submitted in partial fulfilment of the requirement for the degree of

Bachelor of Engineering (Chemical Engineering) (Honours)

JULY 2022

ACKNOWLEDGEMENT

I could not believe I had reached my undergraduate degree's end. These four undergraduate years flew by so fast that I did not even notice it! It still feels like yesterday when I first attended my first ever class in USM in DK5, which is physical chemistry taught by Dr. Irvan Dahlan. Looking back, I was just an ignorant but excited kid trying to understand what on Earth chemical engineering is. So innocent! Here I am, about to graduate as a chemical engineer. I have felt that I have grown so much since I first stepped into USM. As they said, boys become men.

My four undergraduate years are filled with ups and downs, happy and challenging times. As I am writing right now, I am probably stressed by the incoming thesis deadline, but I believe this will be over soon, and my stress will be worth it. This thesis would not be possible without the support of many different essential people, in which I would spare a couple of paragraphs to express my gratitude to them.

I would like to thank the school of chemical engineering, USM, for accepting me into their program. USM lecturers and staff did their best to provide the best education, industrial insights, and facilities to mold all of us to be competent chemical engineers in the real world. Despite the COVID-19 pandemic, I still manage to do my experimental work in time through the staff's fantastic arrangement. I feel so blessed to study chemical engineering at one of the best universities in the world.

Next, I thank the most important person in my FYP: Prof Dr. Lim Jit Kang! "Thank you so much for accepting me as your FYP student." This is the best decision I make in USM to approach him as my FYP advisor. I still remember the email exchanges I had with him discussing the topic of my FYP. He would reply to my question regarding my FYP topic in great length and detail despite his busy schedule. Besides that, he would spare time weekly for literature review discussions, ensuring I was in the right direction. Not every lecturer does that to FYP students! I felt like I had been treated as a postgraduate student that could potentially discover something. That's why he is the best FYP supervisor in USM. I am not exaggerating at all.

Besides that, I would like to extend my gratitude to two graduate students: Mr. Wei Ming and Mr. Wai Hong. They basically babysat me during my laboratory work. Their willingness to answer my questions without hesitation is really much appreciated. I hope all the best to them for their Ph.D. work!

Next, I would like to thank my homies in USM for making my life in USM less stressful. Special shout-out to Goh Jian Loon, Au Jia Yu, Law Ji Pin, and Ng Kah Hoe for the fun times at USM. Being able to joke around with friends helped me to forget my stresses for a while.

Finally, I would like to thank my parents and siblings for their support during my years at USM. I appreciate that my mom continuously checked on me to ensure I was doing okay and gave me moral support through my undergraduate years. I would like to thank my dad, so I do not have to worry about my financials. My dad must cross the border to Singapore every day using a motorcycle – sometimes raining- every day. I hope I made them proud by being the first person in my family to obtain an undergraduate study. I promise I will pay this deed back after graduation!

I am glad I got to experience being a researcher – although working in the unknown realm of knowledge for a short while. I can't wait to start my new chapter in life soon!

James Law Kah Chun
Universiti Sains Malaysia, Engineering Campus
18th June 2022

TABLE OF CONTENTS

LIST OF FIGURES

LIST OF TABLES

LIST OF SYMBOLS

Symbol	Description	Unit
$\vec{F}_m$	Magnetic force acting on single spherical magnetic particle	N
$\vec{M}$	Magnetisation per unit volume	J/Tm^3
$\vec{B}_0$	Inhomogeneous magnetic field	T
r	Radius of particle	m
$\vec{F}_d$	Drag force acting on single particle	N
$\vec{v}$	Velocity of single spherical magnetic particle	m/s
η	Viscosity of the medium	Pas
$\vec{F}_{m\|\|}$	Magnetic force acting parallel to the long axis of rod-shaped magnetic particle	N
$\vec{F}_{m\|\|}$	Drag force acting parallel to the long axis of rod-shaped particle	N
$\overrightarrow{v_{\|\|}}$	Velocity of single rod-shaped magnetic particle moving along its long axis.	m/s
λ_B	Magnetic Bjerrum length	m
λ	Dipole coupling constant	
Γ	Magnetic coupling parameter	
ϕ_0	Volume fraction of particle in a medium	
m	Magnetization modulus	J/T
N^*	Aggregation number	
$U_{Overall}$	Sum of all interparticle interaction energies	J
U_{vdW}	Long-range van der Waals interaction energy	J

Symbol	Description	Unit
U_{elec}	Electric double layer interaction energy	J
U_{mag}	Magnetic attraction energy	J
U_{steric}	Steric interaction energy introduced by polymer coating	J
ΔP	Laplace pressure	Pa
γ	Liquid surface tension	N/m
θ	Contact angle between liquid-air interface and cellulose fibre	
r_p	Average pore radius of the cellulose matrix	m
t	Recorded time	s
R	Distance from drop-point towards the magnet of the stained area	m
V	Volume of droplet	m^3
K	Capillary sorption coefficient	
Λ	$K\left(\frac{\gamma}{\eta}\right)^{u}V^{m}$	
p	Power associated with recorded time	

LIST OF ABBREVIATIONS

IONP	Iron oxide nanoparticle
PSS-70k	Poly(sodium(4)-styrenesulfonate) 70 kDa
DLS	Dynamic light scattering
Fe_2O_4	Iron oxide
NdFeB	Neodymium boron ferrite

ALIRAN BENDALIR MAKROSKOPIK MAGNETOFORESIS KECERUNAN RENDAH MELALUI MATRIKS SELULOSA

ABSTRAK

Dalam kerja ini, kinetik-kinetik aliran bendalir makroskopik dengan larutan oksida besi zarah-zarah nano (IONP) melalui matriks selulosa di bawah medan magnet kecerunan rendah ($< 100\ T/m$) disiasat. Sistem model yang digunakan ialah menitiskan titisan larutan IONP menggunakan empat jenis IONP (nanosfera telanjang, nanosfera bersalut PSS-70k, nanobatang telanjang, dan nanobatang bersalut PSS-70k) di atas Whatman kertas penapis gred 5. Persamaan Gillespie yang diubah suai (model kuasa) telah digunakan untuk memodelkan dua fasa kinetik penyerapan secara jejari dengan takungan cecair terhad. Untuk semua jenis IONP yang digunakan, terdapat kepekatan IONP maksimum yang mempunyai kinetik terpantas dalam setiap fasa penyerapan secara jejari yang mencadangkan kepentingan interaksi antara IONP-IONP dan IONP-serat selulosa dalam memperlahankan aliran bendalir makroskopik melalui matriks selulosa. Perbezaan antara halaju bendalir antara larutan IONP dan larutan kosong yang dikira daripada model kuasa dipasang adalah terlalu pantas yang mencadangkan magnetoforesis kecerunan rendah melalui matriks selulosa harus bersifat kooperatif. Keputusan eksperimen menunjukkan kelebihan salutan PSS-70k untuk meningkatkan kinetik aliran bendalir semasa fasa pertama dan kedua untuk nanobatang. Untuk nanosfera, salutan PSS-70k tidak meningkatkan kinetik fasa kedua. Nanobatang bersalut PSS-70k mempunyai kinetik fasa kedua yang lebih pantas berbanding nanosfera bersalut PSS-70k. Walau bagaimanapun, nanosfera telanjang mempunyai kinetik fasa kedua yang lebih tinggi berbanding dengan nanobatang telanjang. Ini menunjukkan bahawa pengagregatan pantas nanorod telanjang menjadikannya sukar untuk bergerak melalui matriks selulosa. Kajian ini telah memberikan bukti eksperimen

bahawa zarah-zarah nano magnetik boleh meningkatkan kinetik wicking jejari dalam kedua-dua fasa pertama dan kedua melalui matriks selulosa menggunakan medan magnet kecerunan rendah.

MACROSCOPIC FLUID FLOW OF LOW GRADIENT MAGNETOPHORESIS THROUGH CELLULOSE MATRIX

ABSTRACT

In this work, the kinetics of macroscopic fluid flow of iron oxide nanoparticles (IONP) solution through cellulose matrix under low gradient magnetic field ($< 100\, T/m$) are investigated. The modelled system is to drop droplets of IONP solution using four different types of IONP (naked nanospheres, PSS-70k coated nanospheres, naked nanorods, and PSS-70k coated nanorods) onto grade 5 Whatman filter paper. The modified Gillespie equation (power model) is used to model the two phases of radial wicking kinetics with a limited liquid reservoir. For all IONP types used, there is a maximum IONP concentration with the fastest kinetics in each radial wicking phase which suggests the importance of IONP-IONP and IONP-cellulose fibre interactions in slowing down the macroscopic fluid flow through the cellulose matrix. The difference between the fluid velocity between IONP solutions and blank solutions calculated from the fitted power model is too fast, suggesting the low gradient magnetophoresis through the cellulose matrix should be cooperative. Experimental results show the PSS-70k coated nanorods have higher first phase (first phase power: 0.7668) and second phase (second phase power: 0.3458) kinetics compared to its naked counterpart (first phase power: 0.5432; second phase power: 0.1746) . For nanospheres, PSS-70k coating did not improve the second phase kinetics where PSS-70k coated nanospheres (0.2606) has higher second phase power than naked nanospheres (0.1256). PSS-70k coated nanorods (second phase power: 0.3458) have faster second phase kinetics compared to PSS-70k coated nanospheres (second phase power: 0.2606). However, naked nanospheres (second phase power: 0.1256) have higher second-phase kinetics compared to naked nanorods (second phase power: 0.5432). This suggests that the fast aggregation of

naked nanorods made it challenging to move through the cellulose matrix. This study has provided experimental evidence that in coupling with capillary pulling, magnetic nanoparticles could improve the radial wicking kinetics in the first and second phases through cellulose matrix using a low gradient magnetic field.

Chapter 1

Introduction

1.1. Research Background

In recent years, the demand for point-of-care (POC) diagnostics has been increasing, especially in the biomedical, environmental, and food industries (Shangguan *et al.*, 2018). POC diagnostics is any diagnostic technique that could be done at the location of interest without going through labour-intensive laboratory testing. The introduction of microfluidic paper-based analytical devices (μ-PADs) by Martinez and co-workers. (Martinez et al. 2007) was able to meet the growing demand for POC diagnostics.

μ-PADs offer multiple advantages compared to conventional microfluidic channels. μ-PADs are cheap, easy to fabricate, simple to use, disposable, and portable (Shangguan *et al.*, 2018). In addition, the fluid transport is mainly driven passively by the capillary force without external pumps or pressures. This capillary force is provided by the porous nature of paper and the high contact angle (wetting) between water and paper fibres. However, the porous nature of the paper makes it difficult to control the fluid transport and provides relatively slower fluid velocity compared to smooth microfluidic channels.

A possible strategy is imposing a potential external gradient for driving fluid and nanoparticle motion. A promising candidate to do just that is using a low gradient external magnetic field to provide an extra force that could potentially improve fluid velocity and be an active motion control. Magnetic nanoparticles such as magnetite nanoparticles can be dosed in the fluid sample before dropping it on paper. Under the influence of an external magnetic field such as a permanent magnet, magnetic nanoparticles would undergo magnetophoresis in the direction towards the magnet.

Particle migration poses certain challenges, especially through tortuous media like cellulose matrix. Fluid velocity generated by capillary force is slow, around 0.005 cm/s over a distance of 6.2 cm reported by Channon et al., (2018). Besides, cellulose matrix is a very complex porous media with paper fibres randomly interwoven with varying lengths and widths (MacDonald, 2018). Thus, the cellulose matrix creates a tortuous environment, making magnetic nanoparticle migration difficult as an external magnet pulls these particles towards it in a straight line. In addition, the possibility of particles colliding with paper fibres is very high. It may slow down or stops particle migration through the cellulose matrix.

The kinetics of low gradient magnetophoresis through paper is ill-understood. Call and co-workers have recently studied magnetophoresis in microfluidic channels where stacks of paper were used to provide capillary force for fluid transport (Call et. al. 2020) It is possible that the particle migration reported is through the slits between papers rather than through the paper matrix itself. It is because fluid would flow through a larger opening (slits between papers) as it presents the least resistance to fluid flow. Almost no literature report investigates the macroscopic fluid flow of low gradient magnetophoresis through the paper itself. This work aims to understand the kinetics of such a process and eventually implement such a process for biosensing and nano-sensing purposes.

1.2. Problem Statement

The paper-based sensor has been used extensively in many applications, especially biomedical and environmental applications. To date, most paper-based sensors rely on capillary-based processes with little to no other active motion control available. An external magnetic field is a potential candidate for pump-free motion control using magnetic nanoparticles. This scheme may speed up the sensing process or diversify sensing outcomes beyond binary. The transport behaviour of magnetic nanoparticles in cellulose under magnetophoresis is ill-understood as there are almost no literature reports on this modelled system.

It is hypothesized that cooperative magnetophoresis is the main mechanism for the transport behaviour of magnetic nanoparticles through cellulose matrix under an external magnetic field.

1.3. Research Objectives

There are several detailed objectives to answer the identified problem statement.

- To record the macroscopic fluid flow of magnetic nanoparticles through cellulose matrix under an external magnetic.
- To validate the influences of electrostatic stabilization of magnetic nanoparticles under such system.
- To investigate the influences of magnetoshape anisotropy effects on magnetic nanoparticles (nanospheres versus nanorods) on radial wicking kinetics through cellulose matrix.

1.4. Sustainability Elements in this Work

In this work, the low-gradient magnetophoresis through cellulose matrix is investigated using the radial wicking with limited reservoir as the modelled system. The outcome of this work could diversify paper-based sensor strategies beyond relying on capillary force only. The external magnetic field can act as an active motion control where a permanent magnet can be placed in the preferred direction to attract magnetic nanoparticles through the cellulose matrix. This work focuses on the physics of such process without much regard on its potential application. However, the results from this work could potentially be implemented in biosensing or nano-sensing purposes.

Paper-based sensors based on magnetophoresis could work on detecting pollutants in water to improve water management especially in low to medium income countries. This is in line with sustainable development goal (SDG) 6: clean water and sanitation outlined by the United Nations. This work could also be applied on development of sensors in the health or disease detection in humans which is in line with SDG 3: good health and well-being. For example, paper-based technology helped the development of rapid antigen self-test kit for COVID-19 which helped in controlling the spread of COVID-19 among communities. Even though this work does not address the sustainability issues directly, it can support the development of such sensors towards SDGs.

Chapter 2

Literature Review

2.1. Magnetic Nanoparticles

Nanotechnology is any technology developed on a scale of around 10^{-9} m or 1 nm. Nanotechnology has gained traction and revolutionary advancements ever since the idea of nanotechnology was introduced by Nobel laureate Richard Feynman in his famous talk titled “There’s Plenty of Room at the Bottom” in the year 1960 (Feynman, 2011). Nanotechnology has introduced a new kind of material called nanoparticles. Nanoparticles are materials that are at least smaller than 100 nm in at least one dimension (Laurent *et al.*, 2008).

Certain class of nanoparticles (mostly, iron oxides nanoparticles, IONP) could be magnetised under an external magnetic field. This class of nanoparticles is called magnetic nanoparticles. There are many kinds of iron oxide nanoparticles such as magnetite (Fe_3O_4), hematite (α-Fe_3O_4), maghemite (γ-Fe_3O_4), and antiferromagnetic (FeO). Magnetite and hematite are the most promising magnetic nanoparticles due to its proven biocompatibility (Wu, He and Jiang, 2008). Magnetic nanoparticles exhibit very useful and unique properties such as superparamagnetism, high magnetic susceptibility, and low Curie temperature (Wu, He and Jiang, 2008).

2.2. Physics of Magnetic Nanoparticles Under Low Gradient Magnetic Field

Magnetic particles (in particular, magnetite) on the nanoscale exhibit a unique and useful behaviour known as superparamagnetism. Superparamagnetism is a magnetic behaviour where magnetic particles achieve saturated magnetization in a non-zero external magnetic field and has no magnetization at zero external magnetic fields (De Las Cuevas, Faraudo and Camacho, 2008a). Superparamagnetism can be achieved by reducing the magnetic particle size to the point of single magnetic domain particles with energetically unstable magnetisation, usually around 15 nm (Bean and Livingston, 1959; Leong *et al.*, 2020).

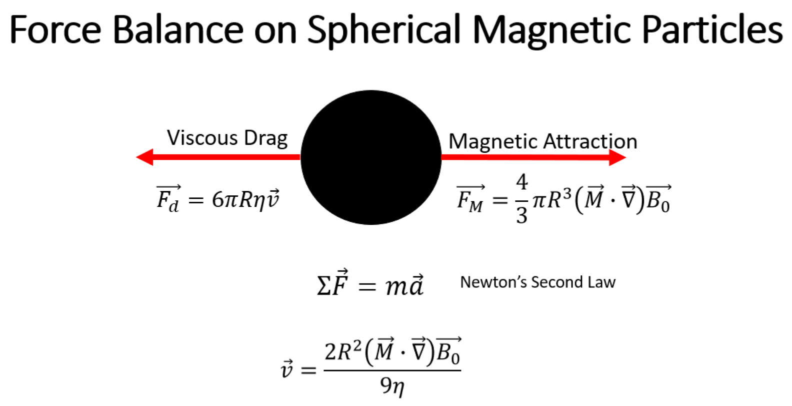

Figure 2.1: Classical Theory of Magnetophoresis. (Drawn by Author)

The phenomenon describing the movement of magnetic nanoparticles under a non-uniform external magnetic field is known as magnetophoresis. The classical theory of magnetophoresis assumes no particle-particle interaction (not even attractive Van der Waals force). Besides that, it assumes that particle motion is restricted to a single layer of stagnant fluid. Thus, there is no hydrodynamic effect except viscous drag acting on the particle.

The magnetic force, $\vec{F}_m$ acting on a single spherical magnetic nanoparticle can be described by the following expression.

$$\vec{F}_m = \frac{4}{3}\pi r^3(\vec{M}\cdot\vec{\nabla})\vec{B}_0 \tag{1}$$

$\vec{M}$ is the magnetisation per unit volume of magnetic nanoparticle, r is the radius of magnetic nanoparticle, and $\vec{B}_0$ is the inhomogeneous magnetic field created by an external magnetic source. A drag force, $\vec{F}_d$ would act on the moving magnetic nanoparticle in a medium described by the Stokes-Einstein equation.

$$\vec{F}_d = 6\pi\eta r\vec{v} \tag{2}$$

$\vec{v}$ is the velocity of spherical magnetic nanoparticle, and η is the viscosity of the medium. The magnetophoretic velocity of the magnetic nanoparticle can be derived by equating these two forces.

$$\vec{v} = \frac{2r^2}{9\eta}(\vec{M} \cdot \vec{\nabla})\vec{B}_0 \tag{3}$$

In this study, particles with high aspect ratio like IONP nanorods are investigated as well. The shape anisotropy of IONP nanorods has a significant effect on its magnetophoretic behaviour due to the difference in drag force.

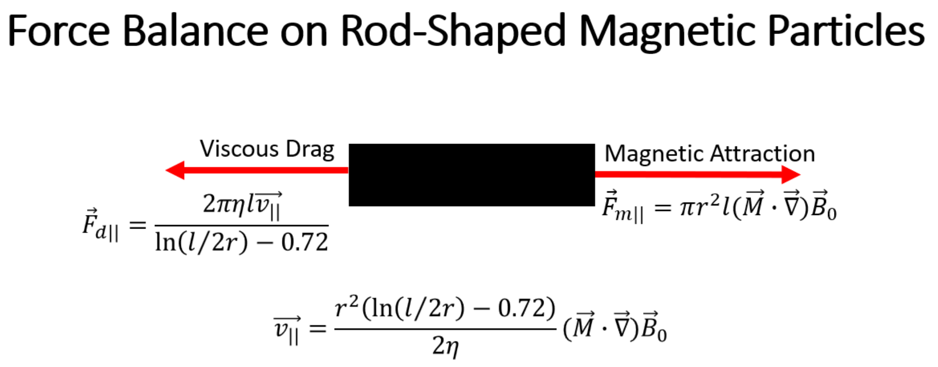

Figure 2.2: Magnetophoretic Velocity for Rod-Shaped Magnetic Particles. (Drawn by Author)

By assuming IONP nanorods with aspect ratio close to 20 are orientated along its long axis parallel with the external magnetic field lines, the drag force acting on IONP nanorods, $\vec{F}_{d||}$ is given by the following expression (Edwards, Engheta and Evoy, 2007).

$$\vec{F}_{d||} = \frac{2\pi\eta l\overrightarrow{v_{||}}}{\ln(l/2r) - 0.72} \tag{4}$$

$\overrightarrow{v_{||}}$ is the magnetophoretic velocity of rod-shaped magnetic nanoparticles, and l is the length of its long axis. The magnetic force, $\vec{F}_{m||}$ acting on a single rod-shaped magnetic nanoparticle can be described by the following expression.

$$\vec{F}_{m||} = \pi r^2 l(\vec{M} \cdot \vec{\nabla})\vec{B}_0 \tag{5}$$

The magnetophoretic velocity of a single IONP nanorod can be obtained by equating equation (4) and (5).

$$\overrightarrow{v_{||}} = \frac{r^2(\ln(l/2r) - 0.72)}{2\eta}(\vec{M} \cdot \vec{\nabla})\vec{B}_0 \tag{6}$$

Lim and co-workers have compared the calculated magnetophoretic velocity using equation (3) and (6) between spherical IONP ($r = 10nm$) and rod-shaped IONP ($r = 10nm; l = 300nm$) (Lim et al., 2009). It has been found that the magnetophoretic velocity of rod-shaped IONP is almost six times larger than spherical IONP. This large difference in magnetophoretic velocity is due to the long length of rod-shaped IONP. The following expression is obtained by taking the ratio between Equation (3) and Equation (6) and assuming that both IONP types have the same radii.

$$\frac{\vec{v}}{\overrightarrow{v_{||}}} = \frac{9}{4(\ln(\alpha/2) - 0.72)} \tag{7}$$

$\alpha = l/r$ is the aspect ratio of the nanoparticles. From equation (7), it is obvious that $\vec{v}/\overrightarrow{v_{||}}$ ratio decreases with increasing aspect ratio for the same radii. From this theoretical analysis alone, it is expected that rod-shaped magnetic nanoparticles would perform better (higher magnetophoretic velocity) compared to their spherical counterpart in magnetophoresis experiments.

A typical magnetophoretic velocity under a low gradient magnetic field ($\nabla B_0 \approx 30\ T/m$) in water environment is around 10^{-7} ms^{-1}. In other words, a particle with this velocity would take approximately 1.16 days to traverse 1 cm! Moreover, its Reynolds number and Peclet Number are 2.52×10^{-8} and 2.24×10^{-4} respectively. Low Reynolds number and Peclet number indicate that viscosity and diffusion effects dominate over magnetophoresis (Lim, Yeap and Low, 2014).

It is well known that magnetic nanoparticles form large particle clusters under a low gradient magnetic field by aligning their magnetic dipoles, which would increase their magnetophoretic velocity. This peculiar phenomenon is known as cooperative magnetophoresis of the magnetic nanoparticle. De Las Cuevas and co-workers have developed a criterion for the occurrence of cooperative magnetophoresis using the dipole coupling constant, λ (De Las Cuevas et al. 2008).

$$\lambda = \left(\frac{\lambda_B}{2r}\right)^3 \tag{8}$$

$\lambda_B = \left(8\pi\mu_0 {M_s}^2/9k_BT\right)^{1/3} r^2$ is the magnetic Bjerrum length defined as the length between two different parallel dipoles such that attractive magnetic energy is equal to the thermal energy. Attractive magnetic energy tends to form particle clusters, while thermal energy tends to disrupt particle cluster formation. This implies that cooperative magnetophoresis occurs when $\lambda > 1$.

Aggregation number, N^* is another useful number defined by the following expression (Andreu, Camacho and Faraudo, 2011).

$$N^* = \sqrt{\phi_0 \exp(\Gamma - 1)} \tag{9}$$

ϕ_0 is the volume fraction of particles in the medium and $\Gamma = \mu_0 m^2/2\pi d^3 k_B T$ is the magnetic coupling parameter which is the ratio between maximum magnetic dipole energy and thermal energy. m is the magnetization modulus defined by $m = MV$, V is the volume of a single IONP, and d is the diameter of the IONP. This parameter can be used as well besides λ to predict whether the magnetic nanoparticles would undergo cooperative magnetophoresis (Leong *et al.*, 2020). Andreu et al. (2011) have shown that N^* is approximately equal to the average length of magnetic nanoparticle aggregate provided N^* is much less than the number concentration of magnetic nanoparticle in the medium.

2.3. Particle Interactions between Magnetic Nanoparticles

The interactions between particles dictates the colloidal stability of the particle system. For magnetic particle systems, the interaction energy between particles can be modelled using the extended Derjaguin-Landau-Verwey-Overbeek (DLVO) theory represented by the following expression (Israelachvili, 2011; Yeap *et al.*, 2012).

$$U_{Overall} = U_{vdW} + U_{elec} + U_{mag} + U_{steric} \tag{10}$$

$U_{Overall}$ is the sum of all interparticle interactions between magnetic particles, U_{vdW} is the long-range van der Waals interaction, U_{elec} is the electric double-layer interaction, U_{mag} is the magnetic attraction between magnetic particles, and U_{steric} is the steric interaction introduced by a polymer coating around the particles. U_{vdW} and U_{mag} are attractive in nature and assign as negative value while U_{elec} and U_{steric} are repulsive in nature and assign as positive value (Israelachvili, 2011). With this convention, positive value for $U_{Overall}$ meant that particles are repulsive to each other while negative value for $U_{Overall}$ meant that particles are attractive to each other.

When $U_{Overall}$ is negative, the particle is said to be colloidally unstable which encourages the formation for large aggregates. When $U_{Overall}$ is positive, the particle is said to be colloidally stable with decreased aggregation rates. The colloidal stability of magnetic nanoparticles can be increased by introducing polymer coating to provide steric hindrance. The works by Yeap and co-workers found that use of PSS-70k coating is effective in improving small clusters of IONP which would be used in this study ((Yeap *et al.*, 2012) .

2.4. Transport Behaviour of Fluids in Cellulose Matrix

The capillary force mainly drives fluid transport in cellulose matrix (or any porous material). Classically, the cellulose matrix can be modelled using bundles of capillaries with a uniform pore radius. Capillary force is induced due to the contact angle formed between water, air, and cellulose fibres, creating a curved liquid-air interface in the cellulose matrix (Boodaghi and Shamloo, 2020a). A pressure difference is formed between the liquid-air interface known as Laplace pressure which drives the liquid flow. It is assumed that the fluid flow is purely driven by capillary force without being subjected to external potential fields except for the gravitation field. However, it can be safely assumed that the gravitation effect on this system is negligible as the amount of fluid used in paper-based experiments is small.

$$\Delta P = \frac{2\gamma \cos\theta}{r_p} \qquad (11)$$

Equation (6) is the expression for the Laplace pressure. γ is the liquid surface tension, θ is the contact angle formed between liquid-air interface and cellulose fibre, and r_p is the average pore radius of the cellulose matrix. By assuming that Laplace pressure is constant, an expression for distance liquid travelled in the cellulose matrix can be obtained using Hagen-Poiseuille equation for laminar flow. The following expression is known as Lucas-Washburn equation.

$$L = \sqrt{\frac{\gamma r t \cos\theta}{2\eta}} \tag{12}$$

L is the distance travelled by the liquid in the cellulose matrix and t is its corresponding time. This equation is suitable for modelling an unlimited reservoir of liquid supplied to the cellulose matrix because it describes that the distance travelled by the liquid, L, will continue to increase as time goes by. This is not true for a system with a limited liquid reservoir where the liquid would stop travelling once the liquid reservoir is used up. Radial wicking of liquid droplets on paper is an example where the liquid reservoir is limited (Marmur, 1992).

In this modelled system, the liquid moves out radially from the point where the droplet is dropped. The fluid transport occurs in two stages (Hertaeg *et al.*, 2020). In the first stage, the liquid rapidly penetrates to large pores of the cellulose matrix with some fraction of the liquid droplet still on the paper surface at the drop point. The second stage occurs when the liquid droplet fully penetrates the matrix. In this second stage, liquid in the large pores (in the centre) redistributes itself into the smaller pores (in the edge) (Marmur, 1992). This redistribution effect creates a negative capillary pressure by forming voids in the central region which ultimately stops the liquid flow.

The radial wicking of liquid droplets can be described by using the modified Gillespie equation as shown below (Kissa, 1981).

$$R(t)^2 = K\left(\frac{\gamma}{\eta}\right)^u V^m t^p \tag{13}$$

γ is the surface tension of the liquid, η is the viscosity of the liquid, V is the volume of the droplet, t is the time of spreading, R is the radius of the stained area, u, m, and p are constants that describes the deviation from the Gillespie equation. $K = 27bq_s \cos\theta / 8h^2c_s^3$ is the capillary sorption coefficient where b is a constant that relates to substate (cellulose matrix is the substrate in this case), q_s is the permeability of the substrate, b is the thickness of the substrate, and c_s is the saturation concentration of liquid in the substrate. Basically, K is a constant that describes the substrate's characteristics, the cellulose matrix. This modified Gillespie equation assumes that the pressure gradient is constant, and Darcy's law holds. If the substrate and liquid used and the volume of the liquid droplet remained unchanged, the modified Gillespie equation can be simplified to the following expression.

$$R(t)^2 = \Lambda t^p;\ \Lambda = K\left(\frac{\gamma}{\eta}\right)^u V^m \tag{14}$$

Equation (13) essentially describes that the liquid radial wicking in substrate can be modelled using a power law. The power, p is always much smaller than unity where it is typically around 0.30 for initially dry substrate (Danino and Marmur, 1994). Since there are two stages in liquid radial wicking, it is expected that the power, p would be different for each stage. For initially wet substrate, this power, p may change which have not been investigated in literature. All in all, the constant, Λ describes characteristics of liquid and substrate used as well as the volume of liquid droplet and the power, p is an empirical constant that describes the deviation from assumption used to derive the Gillespie equation.

2.5. Knowledge Gaps

Many paper-based sensors available for biomedical and environmental applications are mainly based on the utilisation of capillary force. This capillary force allows fluid transport in the cellulose matrix without any external pumps. However, the capillary force acts on the fluid and particles isotropically within the two-dimensional plane of the cellulose matrix. As a result, the fluid and particles spread around the cellulose matrix in all directions equally.

It could be beneficial that the fluid or particles in the matrix could preferentially move in one direction in the two-dimensional plane. A possible way to do that is using magnetic nanoparticles under an external magnetic field. Magnetic nanoparticles can be suspended in the liquid, which would be dropped on the paper. A simple permanent magnet can be placed in the preferred direction to attract these magnetic nanoparticles in the cellulose matrix. The kinetics of such a process is not well-understood, with almost no literature reports on this modelled system.

The closest literature report on this problem is the recent work by Call and co-workers, which demonstrated the possibility of magnetic particle separations using stacks of paper to provide strong enough capillary force for high-velocity flow in a microfluidic channel (Call *et al.*, 2020). However, the modelled system investigated by the author does not investigate the movement of particles inside the cellulose matrix itself.

Recent work by Hertaeg and co-workers investigated the kinetics of radial wicking of biological fluids in cellulose matric such as blood by keeping track of its spatial and temporal evolution (Hertaeg *et al.*, 2020). No literature (to the best of my knowledge) put these two concepts together to investigate magnetophoresis in cellulose matrix.

Under low gradient magnetophoresis, it is known that the magnetic nanoparticles must perform cooperative magnetophoresis to counteract the effect of viscosity under this low Reynolds number regime. Whether cooperative magnetophoresis would even happen under such confined geometry in the cellulose matrix is still a question. Even if it is confirmed that cooperative magnetophoresis happened, the contribution of capillary force versus magnetic force acting on the nanoparticle is not known. This information is important to assess the feasibility of using a magnetic field as active motion control for paper-based sensors.

Chapter 3

Methodology

3.1. Preparation PSS 70k-coated Iron Oxide Nanoparticles

The preparation method used is outlined by (Yeap *et al.*, 2012). Iron oxide nanoparticles suspension (2500 mg/L) in deionized water is prepared by ultrasonification to disperse the aggregates. Another solution containing 0.005 g/mL PSS 70k solution is prepared by ultrasonification for at least 60 minutes for good dispersity of PSS 70k. The PSS 70k concentration is chosen such that it is 500 times more than the estimated amount needed to form a single layer on the iron oxide nanoparticles. These two suspensions (iron oxide nanoparticles and PSS 70k) have its pH adjusted to 3.5-4 before adding the former in the PSS 70k suspension. Iron oxide nanoparticles has an isoelectric point of 6.30 so iron oxide is positively charged while PSS 70k is negatively charged (PSS 70k is negatively charged at all pH values) at pH 3.5-4.0. The physisorption of PSS 70k onto the surface of iron oxide nanoparticles is mainly driven by electrostatic interaction. The physisorption is allowed to sit for 1 day in an end-to-end rotating rack at 37 rpm. After 1 day, the PSS 70k-coated iron oxide nanoparticles are separated using a permanent magnet. It is prewashed before suspending it again in milli-Q water. The washing step is very important to remove the presence of free PSS 70k in the solution which aggregates the particles via depletion force. At the end, a stock IONP solution of 2500 mg/L is produced which can be used to dilute to different IONP concentrations (0, 200, 400, 600, 800, 1000 mg/L).

3.2. Characterization of PSS 70k-Coated and Naked IONP

Dynamic light scattering (DLS) is used to determine the hydrodynamic layer of IONP solution (Lim *et al.*, 2013). The DLS equipment used is Malvern Instrument Zetasizer ZS. For each IONP samples, 20 mg/L of IONP solution is prepared. A dilute solution of IONP is used to prevent multiple scattering and particle-particle interaction during the measurement (Leong, Ahmad and Lim, 2015). During DLS measurement, the IONP solution is exposed to an electromagnetic wave beam (light beam). As these electromagnetic waves approaches IONP, its magnitude and direction change due to a phenomenon called scattering. This scattered light beam is measured 173^0 from the incident light beam. The magnitude of the scattered light beam fluctuates as IONP are in constant Brownian motion. The fluctuation in the intensity of the scattered light beam contains the information regarding the diffusivity coefficient of IONP which can be inferred using the cumulant method. By assuming the IONP is spherical, the Einstein-Stokes equation can be used to determine its hydrodynamic size. By using the same Malvern Instrument Zetasizer ZS, the zeta potential of IONP can be measured as well.

3.3. Droplet Tracing Experimental Set-Up

The experimental set-up to capture the macroscopic evolution of the fluid transport in paper is adopted from experimental set-up designed by Hertaeg et al., (2020). A strip of filter paper (1.5 cm by 3.25 cm) (see Appendix E for the chosen filter paper width justification) is positioned horizontally on top of a glass microscope glass which is held by two retort stands such that the top view of the paper is exposed to air and bottom view of the paper is exposed to glass substrate. The filter paper used is Grade 5 Whatman filter paper with particle retention of 2.5 μm or 2500 nm. A cylindrical neodymium boron ferrite (NdFeB) magnet is placed 1 cm away from the droplet's drop point (see Appendix D for justification on distance of magnet from drop-point) which is held by a third retort stand. A Transferpette is used to produce droplets that contains 10μL onto the filter paper strip. A neodymium magnet is placed 1 cm away from the droplet's drop point. The bottom view of the filter paper is captured using a smartphone camera (Xiaomi Mi A3) with a 45-degree angled mirror placed below the filter paper strip. 45-degree angled mirror is crucial to prevent the image captured being distorted. The smartphone used is held by a tripod stand for video stability. (see Appendix A for further details on experimental set-up) The video captured with 1080p resolution using 60fps. A high fps is used to capture the kinetics of stain area growth in greater resolution. Before starting the experiment, a stock solution of each IONP type (naked nanospheres, PSS-70k coated nanospheres, naked nanorods, PSS-70k coated nanorods) of 2500 mg/L are prepared. For each IONP type, the stock solution is diluted to 200 mg/L, 400 mg/L, 600 mg/L, 800 mg/L, and 1000 mg/L. In each diluted solution, methyl orange is added such that each diluted solution contains 500 mg/L of methyl orange. A relatively high concentration of methyl orange is added to the solution because the droplet must be coloured enough so that the camera could pick up spatial and temporal evolution of the droplet relative to its background (white filter paper). Since methyl orange is an anionic azo dye (Wu *et al.*, 2021) and naked and PSS-70k coated IONP has negatively-charge surface in deionized water from DLS measurement, it is believed that the methyl orange would not adsorbed onto the surface of the IONP due to electrostatic repulsion and be freely suspended in the solution. Even if there is some degree of methyl orange adsorption on IONP surface, methyl orange molecules are over-supplied to ensure freely suspended methyl orange molecules in the solution. (see Appendix B)

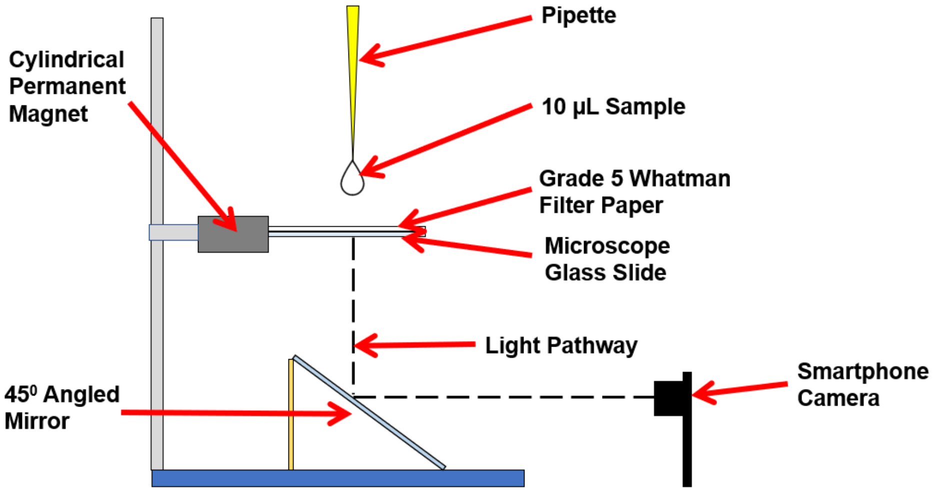

Figure 3.1: Graphical illustration of the droplet tracing experiment set-up. (Side view)

3.4. Droplet Tracing Experimental Procedure

A 2500 mg/L of PSS 70k-coated iron oxide nanoparticle is prepared. A filter paper (Whatman grade 5) is cut into a rectangular strip with the following dimension: 3.25 cm by 1.5 cm. The experimental set-up is discussed in the previous section. A transferpette is used to produce a droplet of the nanoparticle suspension with a volume of 10 μL. Once the paper is set up on the glass slides held by two retort stands, the dry filter paper is wet with 100μL of deionised water. Then, the IONP solution is ultrasonicated for at least 5 mins before transferring a droplet on top of the wetted filter paper. Once the droplet landed on the filter paper strip, the camera is turned on until the stain produced by the droplet in the filter paper reaches plateau. The video captured is saved to be analysed using ImageJ. This step is making sure that IONP is dispersed well in the solution for each experiment. The video is captured for at least 40s where the stain reaches its equilibrium area. The experiment is repeated with the magnet removed. The experiment is repeated by using different IONP concentration (0, 200, 400, 600, 800, 1000 mg/L) and IONP type: 50-100 nm nanospheres, and TODA nanorods. Each data point is repeated three times.

3.5. Droplet Tracing Data Analysis

ImageJ is used as the primary image processing software to extract the kinetics information of the stain growth. For stain growth video, it would be converted to image sequences using Blender which would eventually be processed in ImageJ. In ImageJ, the image sequence would be contrast and turned to black and white image after resizing it using the crop function to reduce the size of the image. The image stack is further process to remove noise using despeckle function. In each image, pixels that correspond to the stain would be counted to give an area. Area in each image would be determined and plotted in stain area versus time plot. Besides tracking the stained area, the distance travelled by the front boundary of the stained area from the drop-point towards the magnet is recorded as well. The image sequences from earlier can be further processed by cropping the bottom half of the stained area. Then, a small vertical rectangle with a width of 0.01 cm and height that fits the images is cropped. The area with dark pixels is recorded for each image sequence. Finally, the area obtained can be divided by 0.01 cm to obtain the distance travelled over time. (see Appendix C for more details on data analysis)

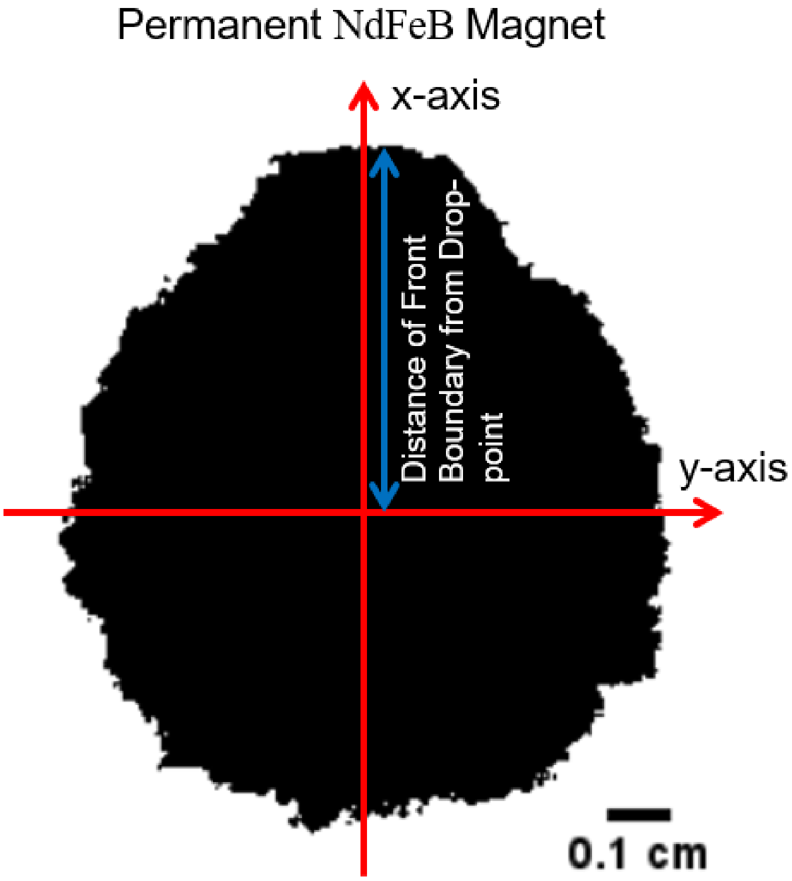

Figure 3.2: Anatomy of data obtained from drop tracing experiment. The top part of the figure shows the location of the permanent magnet. The intersection between two red arrowed lines in the figure shows the drop-point of the sample drop. The double-arrowed blue line shows the distance of the front boundary from the drop-point towards the permanent magnet.

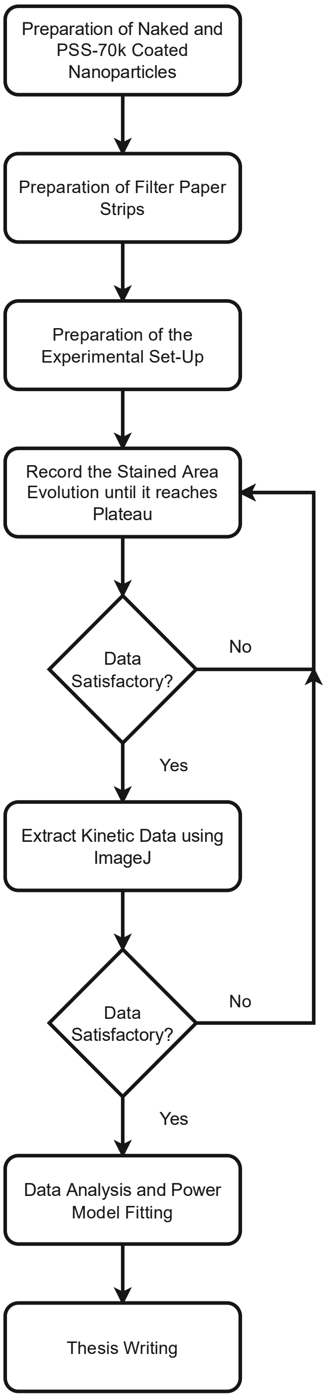

Figure 3.3: Simple flowchart to illustrate the execution of FYP.

Chapter 4

Results and Discussions

4.1. Characterization of IONP Used

There are two types of IONP particles used in this experiment that differs in its geometry: IONP nanospheres from Nanoarmour Structured & Amorphous Materials, Inc. and IONP nanorods from TODA American, Inc.

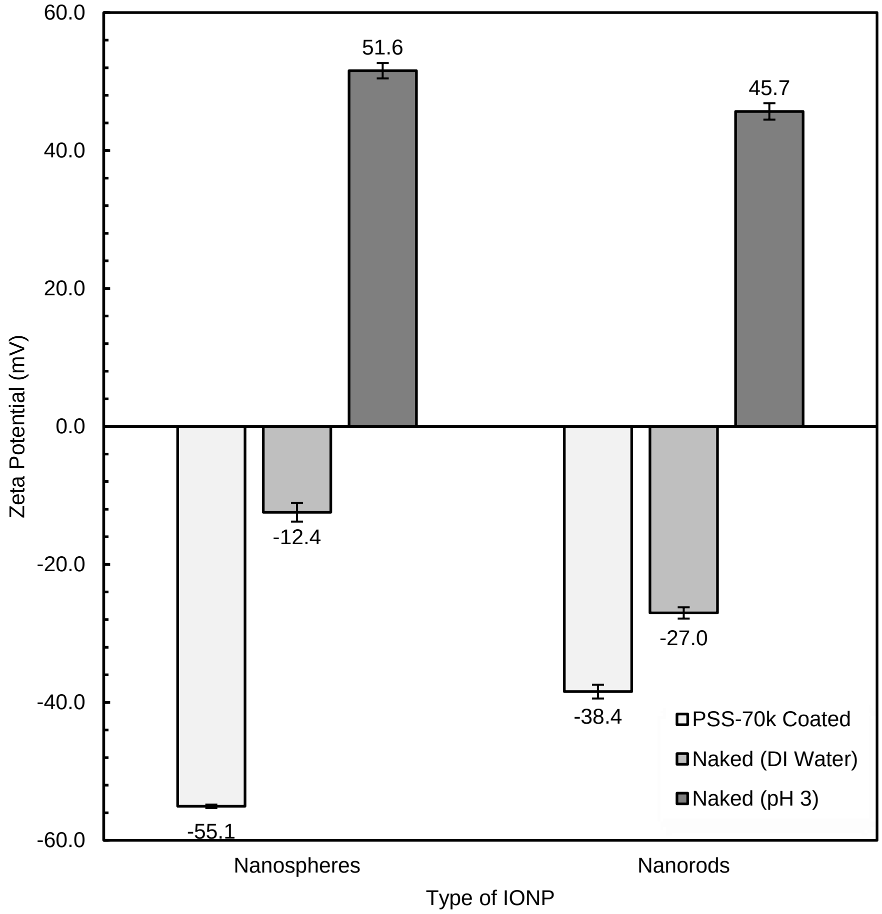

Figure 4.1: Zeta potential of PSS-70k coated IONP nanospheres and nanorods in deionized water as well as its naked counterpart in deionized water and pH 3 solution.

Based on Figure 4.1, both naked IONP nanospheres and nanorods dispersed in deionized water have negatively charged zeta potential of -12.4 ± 1.4 mV and -27.0 ± 0.8 mV respectively. When the acidity of deionized water is adjusted to pH 3, its zeta potential changes to positive value of +51.6 ± 1.1 mV and +45.7 ± 1.2 mV respectively because Fe_2O_4 is amphoteric in nature and has an isoelectric point of ~6.30 (Yeap *et al.*, 2012). This zeta potential measurement confirms that pH 3 environment created during the preparation of PSS-70k coated IONP favours the physisorption of PSS-70k (anionic polymer) on IONP surface by electrostatic attraction. In addition, the zeta potential of IONP nanospheres and nanorods after coating with PSS-70k dispersed in deionized water are more negatively charged than its naked counterparts with values of -55.1 ± 0.3 mV and -38.4 ± 1.0 mV respectively. Both naked and PSS-70k coated IONPs dispersed in deionized water are negatively charged during the experiment. This condition is desired to prevent the possible physisorption of IONPs on the cellulose fibres through electrostatic attraction as cellulose fibres are slightly anionic due to the presence of acidic functional group (BeMiller, 2009).